Composites Science and Technology 167 (2018) 515–521

Contents lists available at ScienceDirect

Composites Science and Technology

journal homepage: www.elsevier.com/locate/compscitech

Graphitic carbon nitride (g-C_3N_4) interfacially strengthened carbon fiber epoxy composites

Bo Song[a,b,**], Tingting Wang[b], Honggang Sun[b], Hu Liu[c,d], Xianmin Mai[e,***], Xiaojing Wang[c,f], Li Wang[b], Ning Wang[g], Yudong Huang[h], Zhanhu Guo[c,*]

[a] Marine College, Shandong University, Weihai, Shandong, 264209, China
[b] School of Mechanical, Electrical & Information Engineering, Shandong University, Weihai, Shandong, 264209, China
[c] Integrated Composites Laboratory (ICL), Department of Chemical & Biomolecular Engineering, University of Tennessee, Knoxville, TN, 37996, USA
[d] National Engineering Research Center for Advanced Polymer Processing Technology, Zhengzhou University, Zhengzhou, Henan, 450002, China
[e] School of Urban Planning and Architecture, Southwest Minzu University, Chengdu, 610041, China
[f] School of Material Science and Engineering, Jiangsu University of Science and Technology, Zhenjiang, Jiangsu, 212003, China
[g] State Key Laboratory of Marine Resource Utilization in South China Sea, Hainan University, Haikou, 570228, China
[h] School of Chemistry and Chemical Engineering, Harbin Institute of Technology, Harbin, Helongjiang, 150001, China

ARTICLE INFO

Keywords:
Carbon fibers
C_3N_4
Surface treatments
Interfacial strength
Fiber/matrix bond
Interphase

ABSTRACT

In-situ synthesis of C_3N_4 on the carbon fiber surface was reported for enhancing interfacial properties of carbon fiber reinforced epoxy resin composite. The formed C_3N_4 on the carbon fiber surface can greatly increase the roughness, polar functional groups and wettability of carbon fiber surface, thereby leading to significant enhancement of interfacial properties of composites. After modification, interlaminar shear strength (ILSS) and interfacial shear strength (IFSS) of carbon fibers composites are increased from 44.3 to 60.7 MPa and from 43.1 to 75.9 MPa, respectively. Moreover, the surface free energy of carbon fibers is increased by 65.6%. The improved interfacial properties endow carbon fiber composites with better mechanical properties, leading to an increased tensile strength of composites from 1063 to 1279 MPa and total absorbed energy of impact experiment from 1.22 to 1.75 J. Meanwhile, the dynamic mechanical properties and hydrothermal aging resistance are also enhanced significantly. The storage modulus increases from 64.3 to 74.1 GPa. The markedly enhancement of interfacial mechanical properties and mechanical properties could be attributed to the improved resin wettability, enhanced mechanical interlocking and increased chemical bonding induced by the existence of C_3N_4 on the carbon fiber surface.

1. Introduction

Carbon fibers (CFs) have been considered as an ideal reinforcement of advanced performance composites due to their superior mechanical properties, low weight, good stability and processing properties, outstanding thermal and electrical properties [1–3]. CFs reinforced epoxy resin materials (CFRERMs) as a potential substitute for traditional structural materials such as metal and concrete have been widely used in aerospace and space engineering, defense industry, transportation, sports, construction and other fields [4–6]. The performance and properties of CFRERMs are determined by many factors, such as reinforcement, matrix and interphase [7–10]. The interphase as a bridge between reinforcement fiber and matrix plays a crucial role in determining the load transfer mechanisms and ultimately the physical, chemical and mechanical properties of advanced fiber-reinforced composite materials [11–16]. Unfortunately, CFs have a poor interfacial adhesion with resin matrix due to their smooth surface and chemical inertness. Poor interfacial adhesion in composites can predispose a component to debonding or delamination, thus leading to catastrophic failure [17–20]. To overcome this problem, surface modification of CF and interfacial manipulation of composites with tailored structures and properties had been extensively researched [21–26].

Up to now, various strategies including surface coating [27], chemical oxidation [28,29], ozone [30–32], plasma treatment [33], high energy irradiation [34] and nanomaterials [35,36] have been developed to improve fiber/matrix adhesion. Among them, an effective

* Corresponding author. University of Tennessee, Knoxville, TN, 37996, USA.
** Corresponding author. Marine College, Shandong University, Weihai, Shandong, 264209, China.
*** Corresponding author. Harbin Institute of Technology, Harbin, Helongjiang, 150001, China.
E-mail addresses: songbosduwh@sdu.edu.cn (B. Song), ydhuang.hit1@aliyun.com (Y. Huang), zguo10@utk.edu (Z. Guo).

https://doi.org/10.1016/j.compscitech.2018.08.031
Received 10 June 2018; Received in revised form 2 August 2018; Accepted 23 August 2018
Available online 29 August 2018

method to ameliorate the interfacial quality of CFRERMs is developing hierarchical (or multiscale) micro/nano reinforcements where nanoscale materials are integrated with CFs [37,38]. In this approach, nanomaterials are grafted or anchored onto the surface of CFs under the action of physical and/or chemical adsorption. These nanomaterials (such as graphene, carbon nanotubes (CNTs), nanoclay, metal oxide nanoparticles, etc.) endow interphase with enlarged contact area, intensified mechanical interlocking, strong chemical bonding and/or local stiffening between the fiber and matrix [39–41]. All these factors benefit improving the stress transfer from strong fillers to the polymer matrix and interfacial properties of the final composites.

Graphitic-based nanomaterials such as CNTs, graphene and graphene oxide were widely used to fabricate hierarchical CFs using different techniques [42,43]. The easiest approach to coat graphitic-based materials onto the CF is surface coating (dip coating and spray coating). This surface coating can effectively protect the fibers against damage or friction, improve the interfacial properties and out-of-plane shear properties of final composites. For example, Zhang et al. [44] deposited CNT networks on CF prepregs using spray coating to improve out-of-plane mechanical properties, and found that Mode-I fracture toughness of the CF laminates was increased by 50% in the presence of 0.047 wt% CNTs. Yao et al. [45] modified CF with CNTs for improving interfacial properties of CF/epoxy composites in a sizing deposition process. The formed gradient interfacial structure in the CF/epoxy composites helped transfer the stress uniformly and made the interlaminar shear strength (ILSS) increased by 13.45%.

Many studies have clearly indicated that the creation of hierarchical CF through CVD is a very straightforward approach for interfacial manipulation [3,4]. In this technique, CNTs are directly grown on the CF surface at high temperature in the presence of catalyst. This results in the improvement of interfacial interlocking, and effective stress transfer between the fibers and matrix [11,46]. However, the high temperature in CVD processes easily led to the deterioration in the tensile properties of CFs, and some catalysts and carbon source were costly and toxic [47]. Qian et al. [42] uniformly grafted CNTs onto Hexcel® IM7 CFs using a CVD method for a better stress transfer between fibers and matrix and the interfacial shear strength (IFSS) was increased by 26%. Meanwhile, an obviously degraded tensile strength of CFs (around 15%) resulted from the observed dissolution of catalyst into the CFs.

Moreover, electrophoretic deposition (EPD) is also a practical and cost-efficient method to fabricate hierarchical composites [38,43]. With the help of EPD, CNTs, graphene and aramid nanofibers (ANFs) were successfully coated on the CF surface and thus improved the surface energy and IFSS. Schaefer et al. [48] deposited carboxylic acid-functionalized carbon nanofibers (O-CNFs) on the surface of single CFs, and these O-CNFs coated CFs provided an IFSS increase of 207.6%. Rodriguez et al. [49] also prepared the hierarchical fabric by depositing oxidized CNFs and amidized CNFs on the surface of CF layers. The relevant composites containing oxidized CNFs or amidized CNFs showed an increase in ILSS of 9.08% and 12.44%, respectively. Sui et al. [50] built a transition layer of oxidized MWCNTs on CFs using a continuous EPD method. The static and fatigue tests showed an increase of 33.3% in IFSS, 10.5 in ILSS, 9.5% in flexural strength, and 15.4% in flexural modulus, respectively.

Chemical reaction is another common strategy to graft graphitic-based nanomaterials onto CFs surface for improved interfacial properties [46,51–53]. In the pioneering research of Islam et al. [54], CNTs were directly grafted onto CFs through ester linkage in the absence of catalyst or coupling agents. Pulling out experiment confirmed the existence of strong carbon-carbon bonding in the interphase, which provided significantly improved interfacial and impact properties. For example, Zhao et al. [51] fabricated a CF/polyhedral oligomeric silsesquioxane (POSS)/CNT hierarchical reinforcement using octaglycidyldimethylsilyl POSS as the linkage between CFs and CNTs. Both the ILSS and impact resistance of final hierarchical composites had a dramatic improvement compared with the composites containing untreated CFs. In another study, He et al. [55] fabricated CNT-CF hierarchical structures using poly-(amidoamine) as a “bridging” in a chemical reaction process. The directly measured grafting strength between individual CNT and CFs substrate varied between the van der Waals (5 MPa) force and 7 times of van der Waals force (90 MPa).

Although numerous methods have been devised for further development of hierarchical reinforcements. But the application of these hierarchical reinforcements is frequently limited by complicated technology and expensive reagents. Therefore, the greatest challenge of hierarchical reinforcements is still searching for a facile and effective approach for improved interfacial properties. In the present work, a facile and effective strategy to fabricate hierarchical carbon fibers is reported for enhanced interfacial properties of CFRERMs through in-situ synthesis of graphitic carbon nitride (g-C_3N_4) on the CF surface. The enhanced effect of g-C_3N_4 on interfacial adhesion is superior to those of the other carbon fiber/epoxy composites (as shown in Table S2). Moreover, surface morphology of CFs and fracture appearance of CFs composites were detected by scanning electron microscope (SEM). Functional groups and chemical elements of CFs and g-C_3N_4 were examined by Fourier Transform Infrared Spectroscopy (FTIR) and X-ray photoelectron spectroscopy (XPS), respectively. Wettability studies were performed on a dynamic contact angle analysis (DCAT). The interfacial properties of CFs composites were evaluated by interlaminar shear strength (ILSS), interfacial shear strength (IFSS), and hydrothermal aging resistance. Meanwhile, the practical application of CFs composites was simulated by dynamic thermomechanical analysis (DMA). As far as we know, there are no relevant research about g-C_3N_4 as reinforcement for improved interfacial properties of fiber/resin composites.

2. Results and discussion

2.1. Surface morphology of carbon fibers

Fig. 1 shows the morphology change of CFs induced by in-situ synthesized g-C_3N_4. Some obvious alterations on the surface morphology were observed. A smooth and neat surface can be found on CFs, and some grooves are uniformly distributed parallel to the fiber axis on the CF surface. After modification, g-C_3N_4 was successfully synthesized and uniformly distributed on the CFs-C_3N_4 surface, which led to the rougher surface.

2.2. Surface chemical elemental composition of carbon fibers

The surface chemical compositions of CFs, C_3N_4 and CFs-C_3N_4 were analyzed by XPS. As illustrated in Table 1, the surface of as-prepared samples contains carbon, nitrogen and oxygen element. The introduction of C_3N_4 causes a sharp increase in nitrogen content on the CFs-C_3N_4 surface. The XPS C1s spectra of samples (Fig. 2) show only a characteristic peak at about 284.6 eV for the CFs which is attributed to the sp^2 hybridized C atoms in the C—C group [56–59]. Meanwhile, pure C_3N_4 exhibits two characteristic peaks at 284.6 and 288.1 eV, respectively. The characteristic peak at 288.1 eV is assigned to the sp^2-bonded C in N═C(—N)$_2$ [60]. After surface modification, XPS C1s spectra of CFs-C_3N_4 show a significant characteristic peak of sp^2-bonded C in the N═C(—N)$_2$ group. These results of XPS analysis confirm the formation of C_3N_4 on the CFs.

The surface functional groups of CFs and C_3N_4 have also been studied by FTIR analysis. As illustrated in Fig. 3, no significant characteristic absorption peak was observed on CFs. After coated with urea, some characteristic absorption peaks of functional groups of urea can be found. The absorption peaks in the range of 3600–3100 cm^{-1} and 900–650 cm^{-1} represent the stretching vibration and in-plane bending vibration of N—H bond, respectively. The characteristic absorption peaks at 1680–1630 cm^{-1} reflect the stretching vibration of the C═O

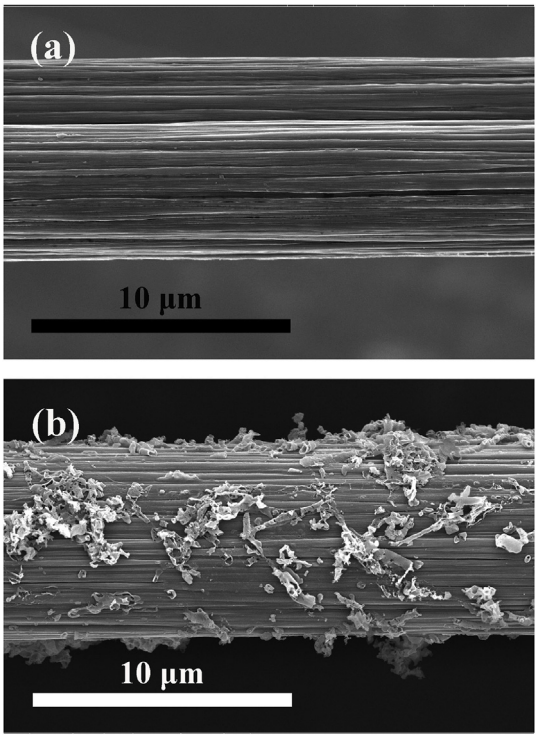

Fig. 1. Surface morphology of carbon fibers: SEM microstructure of (a) CFs; and (b) CFs-C_3N_4.

Table 1
Surface chemical composition of desizing CFs with and without C_3N_4.

Carbon fiber	Element content (%)				
	C	O	N	O/C	N/C
Desizing CFs	83.42	15.27	1.31	18.30	1.57
C_3N_4	43.81	8.05	48.14	18.37	109.88
CFs-C_3N_4	55.21	6.84	37.95	12.39	68.74

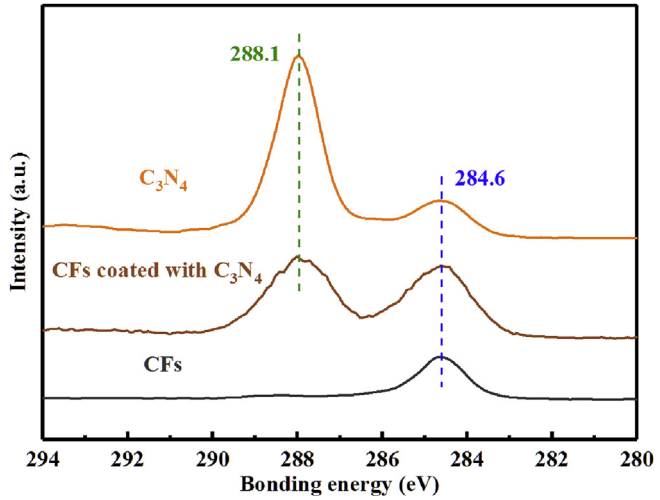

Fig. 2. XPS C1s spectra of CFs, C_3N_4 and CFs-C_3N_4.

bond, and the absorption peaks at 1450 and 1160 cm^{-1} are attributed to the stretching mode and vibration mode of the C—N bond, respectively. For pure C_3N_4, the absorption peaks at around 3500–3000 cm^{-1} were ascribed to the vibration mode of N—H bond and to the stretching mode of O—H bond. The absorption peak at 2178 and 806 cm^{-1} can be

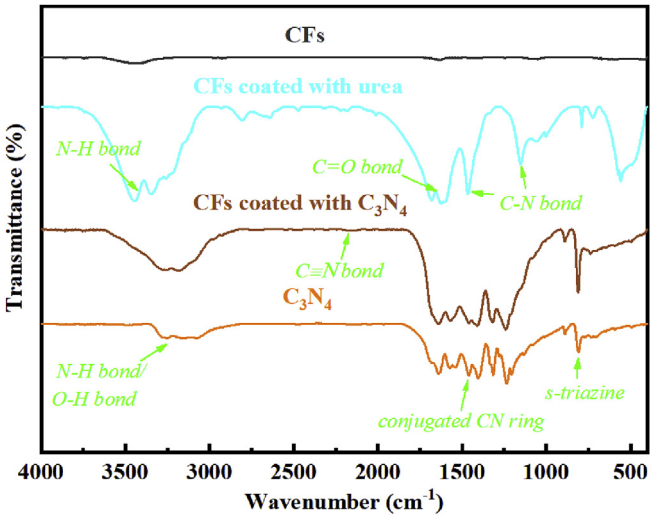

Fig. 3. FTIR spectra of carbon fibers and C_3N_4.

attributed to the C≡N triple bonds and breathing mode of *s*-triazine, respectively [60]. The absorption peaks in the range of 1700–1200 cm^{-1} were assigned to the stretching vibration of conjugated CN rings. In comparison with C_3N_4, the CFs-C_3N_4 sample showed a similar absorption in the wavenumber range of 4000–400 cm^{-1}. The in-situ synthesis of C_3N_4 on CFs can effectively increase the surface functional groups and surface polarity of CFs, thus ameliorate the interfacial wettability and enhance the interfacial adhesion between reinforcement and matrix.

The formation of C_3N_4 on CFs was also confirmed by TGA. Fig. 4 shows the TGA curves. For the CFs sample, a weight loss of 3.72% was observed in the temperature range of 50–800 °C due to thermal degradation of surface materials on the CFs. The TGA curve of CFs-C_3N_4 is similar to that of CFs in the temperature range of 50–500 °C. However, a significant difference between CFs and CFs-C_3N_4 occurred in the temperature range of 500–800 °C owing to the decomposition of C_3N_4. Therefore, CFs-C_3N_4 has a higher weight-loss ratio (4.25%). The above TGA results indicated that the C_3N_4 was synthesized on the CF surface, which was consistent with the XPS and FTIR analysis.

2.3. Dynamic contact angle analysis

The chemical state and topography of the CFs surface influence its surface energy. The high surface energy represents a better wettability

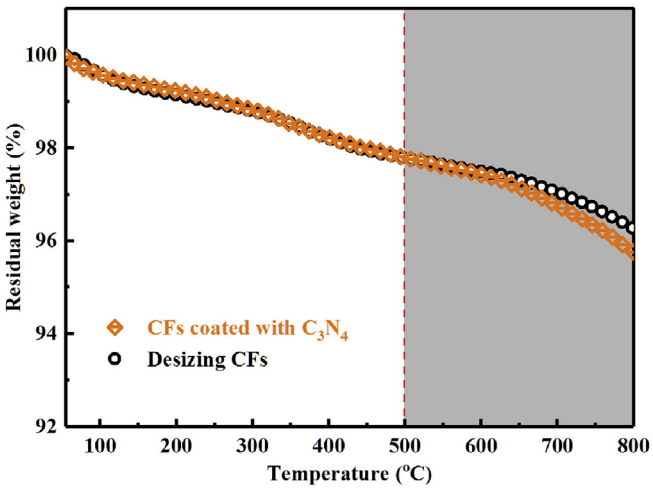

Fig. 4. TGA curves of CFs and CFs-C_3N_4.

Table 2
Contact angle, surface energy and roughness of desizing CFs with and without C_3N_4.

Carbon fibers	Contact angle (°)		Surface energy (mJ/m)		
	Deionized water	Diiodomethane	γ^d	γ^p	γ
Desizing CFs	75.37	59.68	28.75	8.28	37.03
CFs-C_3N_4	46.37	34.45	42.28	19.03	61.31

between CFs and matrix, and strong interfacial adhesion. The surface wettability of CFs was investigated by a Cahn dynamic angle analysis system. Contact angle (θ), surface energy (γ) and its sub-component: dispersion component (γ^d) and polar component (γ^p) of CFs and CFs-C_3N_4 were summarized in Table 2. Compared with CFs, CFs-C_3N_4 possesses smaller contact angles and larger surface energy. The introduced C_3N_4 on the CFs surface causes the contact angle of deionized water (polar solvent) reduced from 75.37° to 46.37°, the contact angle of diiodomethane (non-polar solvent) is decreased from 59.68° to 34.45°, and the surface energy of CFs-C_3N_4 is increased from 37.03 to 61.31 mJ/m. The increased γ^d (from 28.75 to 42.28 mJ/m) and γ^p (from 8.28 to 19.03 mJ/m) could be ascribed to the sharp increase in the surface roughness and functional groups (—NH_2) induced by C_3N_4. Therefore, the hierarchical structure of CFs-C_3N_4 with high surface energy can effectively improve the interfacial wettability between CFs and epoxy resin matrix, thus markedly enhance the interfacial properties (listed in 2.4 and 2.6 section) of the CF composites.

2.4. Interfacial properties evaluation

The interfacial properties has a major impact on the mechanical properties of the final composites. Here, the ILSS as a vital factor of the interface strength of composite laminates was evaluated by short beam bending test (Fig. 5). The ILSS of CFs composites and CFs-C_3N_4 composites is 44.3 and 60.7 MPa, respectively. The introduced C_3N_4 on the CFs surface makes ILSS increase by about 37.2%. The notably enhanced interfacial strength can be attributed to enhanced mechanical interlocking and strong chemical bonding in the interphase. The introduced C_3N_4 endows interphase with bigger contact area, better surface wettability and stronger mechanical interlocking. Meanwhile, open-ring reaction between amino groups on C_3N_4 surface with epoxy groups of matrix creates sufficient chemical bonding between reinforcement and matrix.

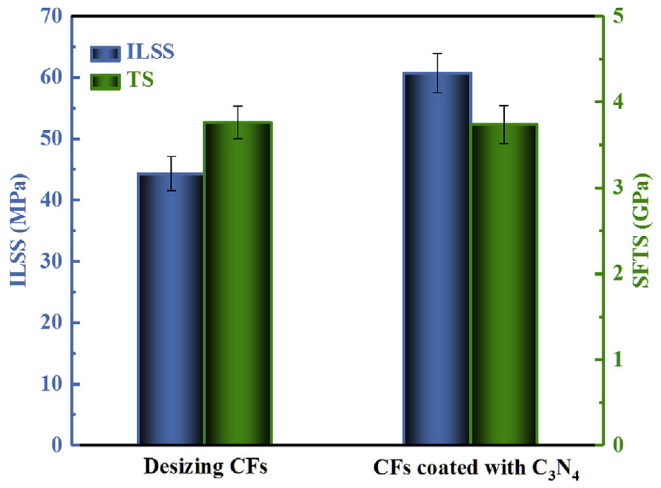

Fig. 5. Tensile strength (TS) of single fiber and ILSS.

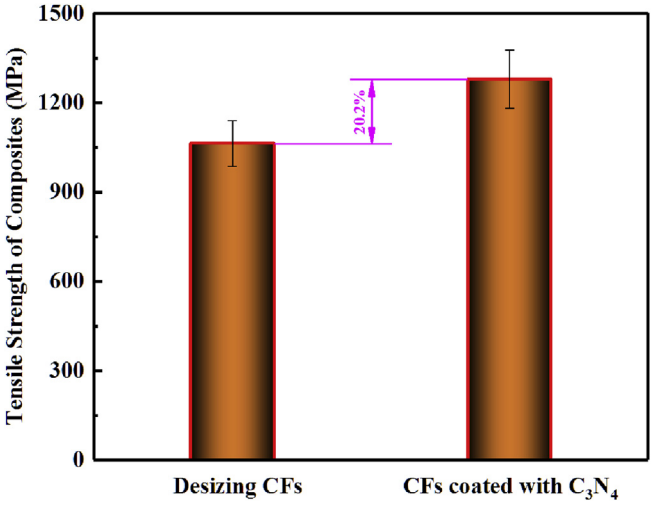

Fig. 6. Tensile strength of composites reinforced with CFs and CFs-C_3N_4, respectively.

2.5. Mechanical properties

The tensile strength (TS) of single fiber was investigated for revealing the effects of surface modification on the inherent mechanical properties of CFs. As illustrated in Fig. 5, the single fiber TS (SFTS) of CFs and CFs-C_3N_4 is 3.76 and 3.74 GPa, respectively. The results of SFTS suggest that the in-situ synthesis of C_3N_4 has no significant effects on the inherent mechanical property of CFs. Moreover, the TS of composites was also studied by unidirectional tensile test of CFs composites and CFs-C_3N_4 composites. As Fig. 6 shows, the C_3N_4 anchored on CFs surface greatly enhances the TS of CFs-C_3N_4 composites. The TS increases from 1063 to 1279 MPa. The markedly improved TS (increased by 20.2%) can be ascribed to the synergistic effects of enhanced mechanical interlocking, wettability and chemical bonding between CFs and epoxy matrix [20]. Meanwhile, the results of mechanical properties test confirm that CFs-C_3N_4 composites have better mechanical properties than those of the as-received CFs composites (as shown in Table S1).

Impact properties as a major embodiment of interfacial property of composites reinforced with CFs and CFs-C_3N_4 were explored. Fig. 7 shows the corresponding results. The initial, propagative and total absorbed energy of CFs composite were 0.24, 0.98 and 1.22 J,

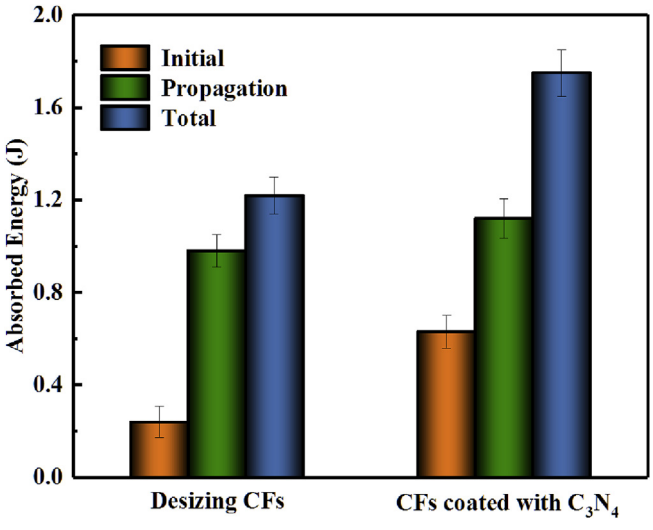

Fig. 7. Impact properties of composites reinforced with CFs and CFs-C_3N_4, respectively.

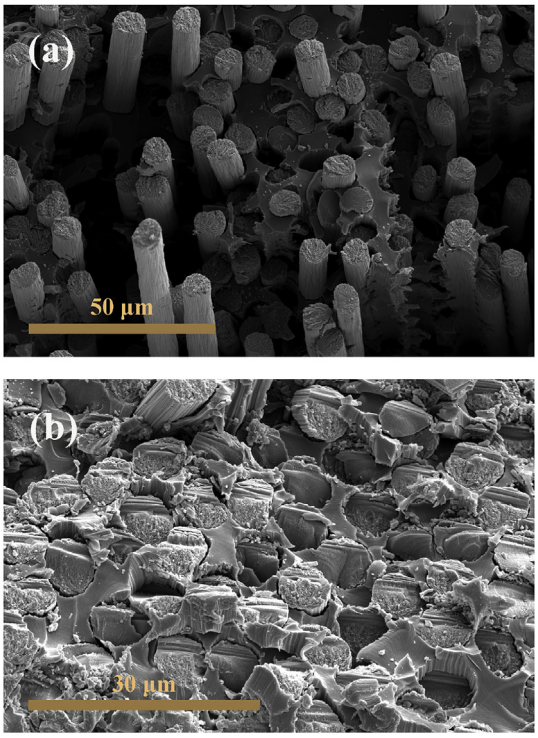

Fig. 8. SEM micrographs of typical failure surfaces for CFs-epoxy composites (a) CFs; and (b) CFs coated with C_3N_4.

respectively. The in-situ formed C_3N_4 on CFs surface effectively enhanced the impact properties of CFs-C_3N_4 composites. The initial, propagative and total absorbed energy of CFs-C_3N_4 composite increased to 0.63, 1.12 and 1.75 J, respectively. The interphase of composites acts as a shielding layer to prevent the crack tips to directly contact the CFs by triggering sub-cracks to absorb the fracture energy. Clearly, the complex interphase structure created by C_3N_4 can trigger more sub-cracks and absorbs more fracture energy, thereby efficiently enhances the impact failure resistance. Meanwhile, the impact fracture surface of CFs composites and CFs-C_3N_4 composites was characterized by SEM, as shown in Fig. 8. For CFs composites, interfacial de-bonding, cracks and pull-out of fiber induced by poor interfacial adhesion are observed on the fracture surface and no resin matrix can be found on the fiber surface. In the case of CFs-C_3N_4 composites, the flat fracture appearance implies a strong and powerful interfacial adhesion created by enhanced mechanical interlocking, better wettability and improved chemical bonding exists in the interfacial area between CFs and epoxy resin matrix.

Fig. 9 depicts the schematic of the impact test model to reveal the

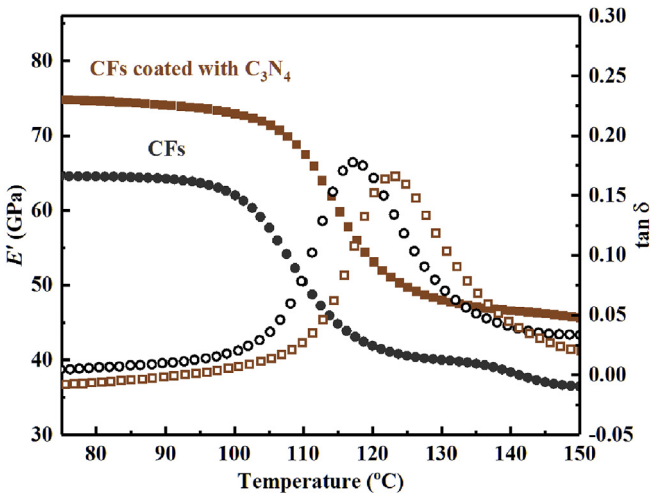

Fig. 10. Dynamic mechanical analysis (DMA) of CFs composites and CFs-C_3N_4 composites.

mechanism of interphase in the composites. The inferior interfacial bonding of CFs composites can result in an ineffective load transfer between CFs and epoxy resin, and fast propagation of cracks along the interphase under a low impact load. Compared to CFs composites, the strong and complicated interfacial structure of CFs-C_3N_4 composites derived from enhanced interfacial chemical bonding and interfacial mechanical interlocking force can markedly improve the interfacial load transfer and release the stress concentration. Meanwhile, the complicated propagation of cracks and enhanced deformation ability of resin led to the formation of micron cracks and change of failure mode. The complex propagation mode of crack consumes more energy, which results in the significantly increased impact properties.

In addition, the dynamic mechanical properties were also studied to simulate the practical applications of composites. Fig. 10 displays the variation of storage modulus (E') and mechanical loss (tan δ) with temperature for the CFs composites and CFs-C_3N_4 composites. Compared with CFs composites, CFs-C_3N_4 composites have a higher E'. The presence of C_3N_4 on the CFs enables E' to increase from 64.3 to 74.1 GPa below T_g (glass transition temperature) and from 36.8 to 45.9 GPa above T_g, which means a better stability of stiffness at higher temperature near T_g. The enhancement of E' was attributed to the higher volume fraction of interphase in the composites and lower mobility of polymer chains at the interphase region. Therefore, the interphase can be considered as additional reinforcement for mechanical stiffening of the composites. Similar phenomenon was also found in the CNTs/CFs composites [39]. Furthermore, the tan δ curves illustrates that CFs-C_3N_4 composites have a higher T_g (122.9 °C) and lower tan δ compared with that of CFs composites (117.4 °C). The increased T_g

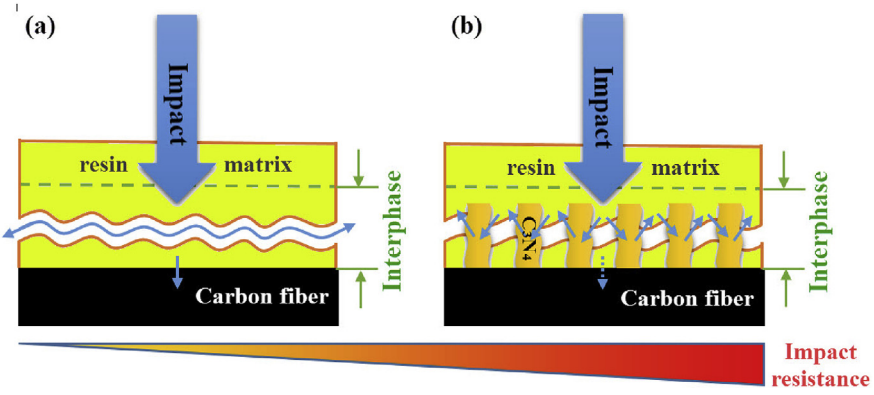

Fig. 9. Schematic impact test of epoxy composites reinforced with CFs and (b) CFs-C_3N_4.

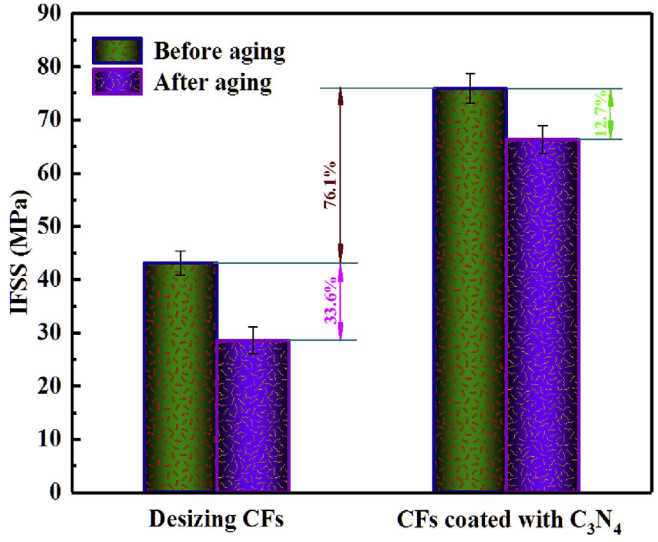

Fig. 11. IFSS before and after hydrothermal aging for 48 h.

could be related to the enhanced restricted-mobility of polymer chains in the interphase region [39]. The amino groups on C_3N_4 can ameliorate the wettability and reaction between fibers and matrix, thereby enhances the crosslink density of interphase [37]. In addition, the C_3N_4 can impede the viscous flow of polymer chains and minimize the energy loss of viscous deformation.

2.6. Hydrothermal aging resistance

High humidity environment can degrade the mechanical properties of composites by the hydrolysis and damage of the interphase structure. Here, the hydrothermal aging resistance of composites reinforced with CFs and CFs-C_3N_4 is also evaluated (Fig. 11). It can be found that the formation of C_3N_4 on CFs results in the IFSS of composite increasing from 43.1 to 75.9 MPa with a growth rate of 76.1%. After hydrothermal aging treatment, the IFSS of CFs and CFs-C_3N_4 composite is reduced by 33.6% and 12.7%, respectively. The interfacial adhesion is poor due to the absence of chemical bond existing in the interphase, thus water molecules can easily penetrate into the interphase, seriously destroys the interfacial structure and obviously degrades the interfacial properties. The enhanced hydrothermal aging resistance of CFs-C_3N_4 composite can be attributed to the stronger interfacial adhesion resulting from enhanced chemical bonds and mechanical interlocking between reinforcements and matrix. Moreover, the damage of C—N bonds formed by opening-ring reaction between amino groups on C_3N_4 surface and epoxy groups of matrix needs more energy, thus protect the interphase from destruction efficiently.

3. Conclusions

g-C_3N_4 was in-situ synthesized on carbon fiber surface for the improvement of interfacial properties between CFs and epoxy matrix. The introduced g-C_3N_4 results in the marked increase of roughness, polar functional groups and surface free energy of CFs surface. The surface free energy of CFs was increased from 37.03 to 61.31 mJ/m. The interfacial properties of carbon fibers composites were significantly improved after modification. The ILSS and IFSS of composites were increased from 44.3 to 60.7 MPa and from 43.1 to 75.9 MPa, respectively. The excellent interfacial properties endued CFs composites with outstanding mechanical properties. The tensile strength of composites was increased from 1063 to 1279 MPa and total absorbed energy of impact experiment was increased from 1.22 to 1.75 J. In addition, the dynamic mechanical properties and hydrothermal aging resistance were also enhanced significantly. The E' of the CFs composites was increased from 64.3 to 74.1 GPa below T_g and from 36.8 to 45.9 GPa above T_g. The hydrothermal aging test demonstrated that the reduction rate of IFSS of CFs composites decreases from 33.6 to 12.7%. The enhanced interfacial properties and mechanical properties of CFs-C_3N_4 were attributed to the improved wettability, enhanced mechanical interlocking and increased chemical bonding. The reported surface modification used in this study can markedly improve the interfacial properties and mechanical properties of carbon fiber composites for other applications like anticorrosion coating and energy storage/conversion units [61–64].

Declaration of interest

The authors declare no conflict of interest regarding the publication of this paper.

Acknowledgment

This work is financially supported by the National Natural Science Foundation of China (Grant Nos. 51603115) and Project funded by China Postdoctoral Science Foundation (Grant Nos. 2017M612266).

Appendix A. Supplementary data

Supplementary data related to this article can be found at https://doi.org/10.1016/j.compscitech.2018.08.031.

References

[1] B. Ashrafi, J. Guan, V. Mirjalili, Y. Zhang, L. Chun, P. Hubert, B. Simard, C.T. Kingston, O. Bourne, A. Johnston, Enhancement of mechanical performance of epoxy/carbon fiber laminate composites using single-walled carbon nanotubes, Compos. Sci. Technol. 71 (13) (2011) 1569–1578.
[2] C.L. Arnold, K.M. Beggs, D.J. Eyckens, F. Stojcevski, L. Servinis, L.C. Henderson, Enhancing interfacial shear strength via surface grafting of carbon fibers using the Kolbe decarboxylation reaction, Compos. Sci. Technol. 159 (2018) 135–141.
[3] F. An, C. Lu, J. Guo, S. He, H. Lu, Y. Yang, Preparation of vertically aligned carbon nanotube arrays grown onto carbon fiber fabric and evaluating its wettability on effect of composite, Appl. Surf. Sci. 258 (3) (2011) 1069–1076.
[4] Z. Zhao, R. Guan, J. Zhang, Z. Zhao, P. Bai, Effects of process parameters of semi-solid stirring on microstructure of Mg-3Sn-1Mn-3SiC (wt%) strip processed by rheo-rolling, Acta Metall. Sin. (Engl. Lett.) 30 (2017) 66–72.
[5] B. Demir, K.M. Beggs, B.L. Fox, L. Servinis, L.C. Henderson, T.R. Walsh, A predictive model of interfacial interactions between functionalised carbon fibre surfaces cross-linked with epoxy resin, Compos. Sci. Technol. 159 (2018) 127–134.
[6] Z. Zhao, P. Bai1, R. Guan, V. Murugadoss, H. Liu, X. Wang, Z. Guo, Microstructural evolution and mechanical strengthening mechanism of Mg-3Sn-1Mn-1La alloy after heat treatments, Mater. Sci. Eng. A 734 (2018) 200–209.
[7] Z. Wu, H. Cui, L. Chen, D. Jiang, L. Weng, Y. Ma, X. Li, X. Zhang, H. Liu, N. Wang, J. Zhang, Y. Ma, M. Zhang, Y. Huang, Z. Guo, Interfacially reinforced unsaturated polyester carbon fiber composites with a vinyl ester-carbon nanotubes sizing agent, Compos. Sci. Technol. 164 (2018) 195–203.
[8] Q. Luo, H. Chen, Y. Lin, H. Du, Q. Hou, F. Hao, N. Wang, Z. Guo, J. Huang, Discrete iron(III) oxide nanoislands for efficient and photostable perovskite solar cells, Adv. Funct. Mater. 27 (34) (2017) 1702090–1702097.
[9] Q. Luo, H. Ma, F. Hao, Q. Hou, J. Ren, L. Wu, Z. Yao, Y. Zhou, N. Wang, K. Jiang, H. Lin, Z. Guo, Carbon nanotube based inverted flexible perovskite solar cells with all-inorganic charge contacts, Adv. Funct. Mater. 27 (42) (2017) 1703068–1703076.
[10] T. Liu, K. Yu, L. Gao, H. Chen, N. Wang, L. Hao, T. Li, H. He, Z. Guo, A graphene quantum dot decorated $SrRuO_3$ mesoporous film as an efficient counter electrode for high-performance dye-sensitized solar cells, J. Mater. Chem. A 5 (34) (2017) 17848–17855.
[11] H. Wu, X. Huang, L. Qian, Recent progress on the metacompoistes with carbonaceous fillers, Eng. Sci. 2 (2018) 17–25, https://doi.org/10.30919/es8d656.
[12] S. Sun, L. Zhu, X. Liu, L. Wu, K. Dai, C. Liu, C. Shen, X. Guo, G. Zheng, Z. Guo, Superhydrophobic shish-kebab membrane with self-cleaning and oil/water separation properties, ACS Sustain. Chem. Eng. (2018), https://doi.org/10.1021/acssuschemeng.8b01047.
[13] C. Wang, B. Mo, Z. He, X. Xie, C.X. Zhao, L. Zhang, Q. Shao, X. Guo, E.K. Wujcik, Z. Guo, Hydroxide ions transportation in polynorbornene anion exchange membrane, Polymer 138 (2018) 363–368.
[14] C. Wang, M. Zhao, J. Li, J. Yu, S. Sun, S. Ge, X. Guo, F. Xie, B. Jiang, E.K. Wujcik, Y. Huang, N. Wang, Z. Guo, Silver nanoparticles/graphene oxide decorated carbon fiber synergistic reinforcement in epoxy-based composites, Polymer 131 (2017) 263–271.
[15] P. Xie, Z. Wang, Z. Zhang, R. Fan, C. Cheng, H. Liu, Y. Liu, T. Li, C. Yan, N. Wang, Z. Guo, Silica microsphere templated self-assembly of a three-dimensional carbon

network with stable radio-frequency negative permittivity and low dielectric loss, J. Mater. Chem. C 6 (19) (2018) 5239–5249.
[16] K. Zhang, G.-H. Li, L.-M. Feng, N. Wang, J. Guo, K. Sun, K.-X. Yu, J.-B. Zeng, T. Li, Z. Guo, M. Wang, Ultralow percolation threshold and enhanced electromagnetic interference shielding in poly(l-lactide)/multi-walled carbon nanotube nanocomposites with electrically conductive segregated networks, J. Mater. Chem. C 5 (36) (2017) 9359–9369.
[17] J. Gao, W. Li, H. Shi, M. Hu, R.K.Y. Li, Preparation, morphology, and mechanical properties of carbon nanotube anchored polymer nanofiber composite, Compos. Sci. Technol. 92 (2014) 95–102.
[18] Y. Li, B. Zhou, G. Zheng, X. Liu, T. Li, C. Yan, C. Cheng, K. Dai, C. Liu, C. Shen, Z. Guo, Continuously prepared highly conductive and stretchable SWNT/MWNT synergistically composited electrospun thermoplastic polyurethane yarns for wearable sensing, J. Mater. Chem. C 6 (9) (2018) 2258–2269.
[19] J. Lin, X. Chen, C. Chen, J. Hu, C. Zhou, X. Cai, W. Wang, C. Zheng, P. Zhang, J. Cheng, Z. Guo, H. Liu, Durably antibacterial and bacterially antiadhesive cotton fabrics coated by cationic fluorinated polymers, ACS Appl. Mater. Interfaces 10 (7) (2018) 6124–6136.
[20] H. Liu, W. Huang, X. Yang, K. Dai, G. Zheng, C. Liu, C. Shen, X. Yan, J. Guo, Z. Guo, Organic vapor sensing behaviors of conductive thermoplastic polyurethane–graphene nanocomposites, J. Mater. Chem. C 4 (20) (2016) 4459–4469.
[21] N. Wu, C. Liu, D. Xu, J. Liu, W. Liu, Q. Shao, Z. Guo, Enhanced electromagnetic wave absorption of three-dimensional porous Fe_3O_4/C composite flowers, ACS Sustain. Chem. Eng. (2018), https://doi.org/10.1021/acssuschemeng.8b03097.
[22] Z. Hu, D. Zhang, F. Lu, W. Yuan, X. Xu, Q. Zhang, H. Liu, Q. Shao, Z. Guo, Y. Huang, Multistimuli-responsive intrinsic self-healing epoxy resin constructed by host–guest interactions, Macromolecules 51 (2018) 5294–5303.
[23] J. Huang, Y. Li, Y. Cao, F. Peng, Y. Cao, Q. Shao, H. Liu, Z. Guo, Hexavalent chromium removal over magnetic carbon nanoadsorbents: synergistic effect of fluorine and nitrogen co-doping, J. Mater. Chem. A 6 (27) (2018) 13062–13074.
[24] H. Kang, Z. Cheng, H. Lai, H. Ma, Y. Liu, X. Mai, Y. Wang, Q. Shao, L. Xiang, X. Guo, Z. Guo, Superlyophobic anti-corrosive and self-cleaning titania robust mesh membrane with enhanced oil/water separation, Separ. Purif. Technol. 201 (2018) 193–204.
[25] Y. Kong, Y. Li, G. Hu, J. Lin, D. Pan, D. Dong, E. Wujick, Q. Shao, M. Wu, J. Zhao, Z. Guo, Preparation of polystyrene-b-poly(ethylene/propylene)-b-polystyrene grafted glycidyl methacrylate and its compatibility with recycled polypropylene/recycled high impact polystyrene blends, Polymer 145 (2018) 232–241.
[26] Y. Li, X. Wu, J. Song, J. Li, Q. Shao, N. Cao, N. Lu, Z. Guo, Reparation of recycled acrylonitrile- butadiene-styrene by pyromellitic dianhydride: reparation performance evaluation and property analysis, Polymer 124 (2017) 41–47.
[27] C. Hu, Z. Li, Y. Wang, J. Gao, K. Dai, G. Zheng, C. Liu, C. Shen, H. Song, Z. Guo, Comparative assessment of the strain-sensing behaviors of polylactic acid nanocomposites: reduced graphene oxide or carbon nanotubes, J. Mater. Chem. C 5 (9) (2017) 2318–2328.
[28] D. Jiang, L. Xing, L. Liu, S. Sun, Q. Zhang, Z. Wu, X. Yan, J. Guo, Y. Huang, Z. Guo, Enhanced mechanical properties and anti-hydrothermal ageing behaviors of unsaturated polyester composites by carbon fibers interfaced with POSS, Compos. Sci. Technol. 117 (2015) 168–175.
[29] P. Xie, F. Dang, B. He, J. Lin, R. Fan, C. Hou, H. Liu, J.-x. Zhang, Y. Ma, Z. Guo, Biogel derived nickel/carbon nanocomposites with enhanced microwave absorption, J. Mater. Chem. C 6 (2018) 8812–8822.
[30] J. Karger-Kocsis, H. Mahmood, A. Pegoretti, Recent advances in fiber/matrix interphase engineering for polymer composites, Prog. Mater. Sci. 73 (2015) 1–43.
[31] Y. Guo, G. Xu, X. Yang, K. Ruan, T. Ma, Q. Zhang, J. Gu, Y. Wu, H. Liu, Z. Guo, Significantly enhanced and precisely modeled thermal conductivity in polyimide nanocomposites with chemically modified graphene via in situ polymerization and electrospinning-hot press technology, J. Mater. Chem. C 6 (12) (2018) 3004–3015.
[32] X. Guan, G. Zheng, K. Dai, C. Liu, X. Yan, C. Shen, Z. Guo, Carbon nanotubes-adsorbed electrospun PA66 nanofiber bundles with improved conductivity and robust flexibility, ACS Appl. Mater. Interfaces 8 (22) (2016) 14150–14159.
[33] K.J. Kim, W.R. Yu, J.H. Youk, J. Lee, Degradation and healing mechanisms of carbon fibers during the catalytic growth of carbon nanotubes on their surfaces, ACS Appl. Mater. Interfaces 4 (4) (2012) 2250–2258.
[34] N. Koutroumanis, A.C. Manikas, P.N. Pappas, F. Petropoulos, L. Sygellou, D. Tasis, K. Papagelis, G. Anagnostopoulos, C. Galiotis, A novel mild method for surface treatment of carbon fibres in epoxy-matrix composites, Compos. Sci. Technol. 157 (2018) 178–184.
[35] X. Zhang, O. Alloul, Q. He, J. Zhu, M.J. Verde, Y. Li, S. Wei, Z. Guo, Strengthened magnetic epoxy nanocomposites with protruding nanoparticles on the graphene nanosheets, Polymer 54 (2013) 3594–3604.
[36] Y. Li, Q. Peng, X. He, P. Hu, C. Wang, Y. Shang, R. Wang, W. Jiao, H. Lv, Synthesis and characterization of a new hierarchical reinforcement by chemically grafting graphene oxide onto carbon fibers, J. Mater. Chem. 22 (36) (2012) 18748–18752.
[37] H. Zhao, L. Chen, J. Yun, L. Tang, Z. Wen, X. Zhang, J. Gu, Improved thermal stabilities, ablation and mechanical properties for carbon fibers/phenolic resins laminated composites modified by silicon-containing polyborazine, Eng. Sci. 2 (2018) 57–66, https://doi.org/10.30919/es8d726.
[38] M. Mehdikhani, A. Matveeva, M.A. Aravand, B.L. Wardle, S.V. Lomov, L. Gorbatikh, Strain mapping at the micro-scale in hierarchical polymer composites with aligned carbon nanotube grafted fibers, Compos. Sci. Technol. 137 (2016) 24–34.
[39] J. Zhao, L. Wu, C. Zhan, Q. Shao, Z. Guo, L. Zhang, Overview of polymer nanocomposites: computer simulation understanding of physical properties, Polymer 133 (2017) 272–287.
[40] Q. Peng, X. He, Y. Li, C. Wang, R. Wang, P. Hu, Y. Yan, T. Sritharan, Chemically and uniformly grafting carbon nanotubes onto carbon fibers by poly(amidoamine) for enhancing interfacial strength in carbon fiber composites, J. Mater. Chem. 22 (13) (2012) 5928–5931.
[41] J. Zhang, Y. Liang, X. Wang, H. Zhou, S. Li, J. Zhang, Y. Feng, N. Lu, Q. Wang, Z. Guo, Strengthened epoxy resin with hyperbranched polyamine-ester anchored graphene oxide via novel phase transfer approach, Adv. Compos Hybrid Mater. 1 (2016) 300–309.
[42] H. Qian, A. Bismarck, E.S. Greenhalgh, M.S.P. Shaffer, Carbon nanotube grafted carbon fibres: a study of wetting and fibre fragmentation, Compos Part A: Appl. S. 41 (9) (2010) 1107–1114.
[43] H. Qian, E.S. Greenhalgh, M.S.P. Shaffer, A. Bismarck, Carbon nanotube-based hierarchical composites: a review, J. Mater. Chem. 20 (23) (2010) 4751–4762.
[44] H. Zhang, Y. Liu, M. Kuwata, E. Bilotti, T. Peijs, Improved fracture toughness and integrated damage sensing capability by spray coated CNTs on carbon fibre prepreg, Compos Part A: Appl. S. 70 (2015) 102–110.
[45] H. Yao, X. Sui, Z. Zhao, Z. Xu, L. Chen, H. Deng, Y. Liu, X. Qian, Optimization of interfacial microstructure and mechanical properties of carbon fiber/epoxy composites via carbon nanotube sizing, Appl. Surf. Sci. 347 (2015) 583–590.
[46] B. Song, T. Wang, H. Sun, Q. Shao, J. Zhao, K. Song, L. Hao, L. Wang, Z. Guo, Two-step hydrothermally synthesized carbon nanodots/WO3 photocatalysts with enhanced photocatalytic performance, Dalton Trans. 46 (45) (2017) 15769–15777.
[47] W. Xia, X. Chen, S. Kundu, X. Wang, G. Grundmeier, Y. Wang, M. Bron, W. Schuhmann, M. Muhler, Chemical vapor synthesis of secondary carbon nanotubes catalyzed by iron nanoparticles electrodeposited on primary carbon nanotubes, Surf. Coating. Technol. 201 (22–23) (2007) 9232–9237.
[48] J.D. Schaefer, A.J. Rodriguez, M.E. Guzman, C.-S. Lim, B. Minaie, Effects of electrophoretically deposited carbon nanofibers on the interface of single carbon fibers embedded in epoxy matrix, Carbon 49 (8) (2011) 2750–2759.
[49] A.J. Rodriguez, M.E. Guzman, C.-S. Lim, B. Minaie, Mechanical properties of carbon nanofiber/fiber-reinforced hierarchical polymer composites manufactured with multiscale-reinforcement fabrics, Carbon 49 (3) (2011) 937–948.
[50] X. Sui, J. Shi, H. Yao, Z. Xu, L. Chen, X. Li, M. Ma, L. Kuang, H. Fu, H. Deng, Interfacial and fatigue-resistant synergetic enhancement of carbon fiber/epoxy hierarchical composites via an electrophoresis deposited carbon nanotube-toughened transition layer, Composer Part A: Appl. S. 92 (2017) 134–144.
[51] F. Zhao, Y. Huang, L. Liu, Y. Bai, L. Xu, Formation of a carbon fiber/polyhedral oligomeric silsesquioxane/carbon nanotube hybrid reinforcement and its effect on the interfacial properties of carbon fiber/epoxy composites, Carbon 49 (8) (2011) 2624–2632.
[52] J. Zhao, J. Chen, S. Xu, M. Shao, D. Yan, M. Wei, D.G. Evans, X. Duan, CoMn-layered double hydroxide nanowalls supported on carbon fibers for high-performance flexible energy storage devices, J. Mater. Chem. A 1 (31) (2013) 8836–8843.
[53] M. Zhao, L. Meng, L. Ma, L. Ma, X. Yang, Y. Huang, J.E. Ryu, A. Shankar, T. Li, C. Yan, Z. Guo, Layer-by-layer grafting CNTs onto carbon fibers surface for enhancing the interfacial properties of epoxy resin composites, Compos. Sci. Technol. 154 (2018) 28–36.
[54] M.S. Islam, Y. Deng, L. Tong, S.N. Faisal, A.K. Roy, A.I. Minett, V.G. Gomes, Grafting carbon nanotubes directly onto carbon fibers for superior mechanical stability: towards next generation aerospace composites and energy storage applications, Carbon 96 (2016) 701–710.
[55] X. He, C. Wang, L. Tong, R. Wang, A. Cao, Q. Peng, S. Moody, Y. Li, Direct measurement of grafting strength between an individual carbon nanotube and a carbon fiber, Carbon 50 (10) (2012) 3782–3788.
[56] X. Shen, T. Zhang, P. Xu, L. Zhang, J. Liu, Z. Chen, Growth of C 3 N 4 nanosheets on carbon-fiber cloth as flexible and macroscale filter-membrane-shaped photocatalyst for degrading the flowing wastewater, Appl. Catal. B Environ. 219 (2017) 425–431.
[57] C. Wang, J. Li, J. Yu, S. Sun, X. Li, F. Xie, B. Jiang, G. Wu, F. Yu, Y. Huang, Grafting of size-controlled graphene oxide sheets onto carbon fiber for reinforcement of carbon fiber/epoxy composite interfacial strength, Composer Part A: Appl. S. 101 (2017) 511–520.
[58] H. Chen, Y. Liu, B. Ren, Y. Zhang, J. Ma, L. Xu, Q. Chen, J. Zheng, Super bulk and interfacial toughness of physically crosslinked double-network hydrogels, Adv. Funct. Mater. 27 (44) (2017) 1703086–1703094.
[59] H. Chen, F. Yang, Q. Chen, J. Zheng, A novel design of multi-mechanoresponsive and mechanically strong hydrogels, Adv. Mater. 29 (21) (2017) 1606900–1606908.
[60] H. Chen, F. Yang, R. Hu, M. Zhang, B. Ren, X. Gong, J. Ma, B. Jiang, Q. Chen, J. Zheng, A comparative study of the mechanical properties of hybrid double-network hydrogels in swollen and as-prepared states, J. Mater. Chem. B 4 (35) (2016) 5814–5824.
[61] Y. Zhang, M. Zhao, J. Zhang, Q. Shao, J. Li, H. Li, B. Lin, M. Yu, S. Chen, Z. Guo, Excellent corrosion protection performance of epoxy composite coatings filled with silane functionalized silicon nitride, J. Polym. Res. 25 (2018) 130.
[62] X. Cui, G. Zhu, Y. Pan, Q. Shao, C. Zhao, M. Dong, Y. Zhang, Z. Guo, Polydimethylsiloxane-titania nanocomposite coating: fabrication and corrosion resistance, Polymer 138 (2018) 203–210.
[63] C. Wang, B. Mo, Z. He, C.X. Zhao, L. Zhang, Q. Shao, X. Guo, E. Wujcik, Z. Guo, Hydroxide ions transportation in polynorbornene anion exchange membrane, Polymer 138 (2018) 363–368.
[64] Z. Wang, R. Wei, J. Gu, H. Liu, C. Liu, C. Luo, J. Kong, Q. Shao, N. Guo, X. Liu, Ultralight, highly compressible and fire-retardant graphene aerogel with self-adjustable electromagnetic wave absorption, Carbon 139 (2018) 1126–1135.